PNAS RESEARCH ARTICLE | CHEMISTRY

Continuous ammonia synthesis from water and nitrogen via contact electrification

Juan Li[a], Yu Xia[a,b,1], Xiaowei Song[b], Bolei Chen[a,1], and Richard N. Zare[b,1]

Edited by Joseph Francisco, University of Pennsylvania, Philadelphia, PA; received October 25, 2023; accepted December 1, 2023

We synthesized ammonia (NH_3) by bubbling nitrogen (N_2) gas into bulk liquid water (200 mL) containing 50 mg polytetrafluoroethylene (PTFE) particles (~5 μm in diameter) suspended with the help of a surfactant (Tween 20, ~0.05 vol.%) at room temperature (25 °C). Electron spin resonance spectroscopy and density functional theory calculations reveal that water acts as the proton donor for the reduction of N_2. Moreover, isotopic labeling of the N_2 gas shows that it is the source of nitrogen in the ammonia. We propose a mechanism for ammonia generation based on the activation of N_2 caused by electron transfer and reduction processes driven by contact electrification. We optimized the pH of the PTFE suspension at 6.5 to 7.0 and employed ultrasonic mixing. We found an ammonia production rate of ~420 μmol L^{-1} h^{-1} per gram of PTFE particles for the conditions described above. This rate did not change more than 10% over an 8-h period of sustained reaction.

ammonia | contact electrification | water

Significance

The Haber–Bosch process for the synthesis of ammonia is one of the important reactions that affect the development of human civilization. Nevertheless, finding a hydrogen source other than methane is receiving much attention for making a more sustainable planet. A previous study demonstrated that ammonia can be synthesized from N_2 by spraying water microdroplets onto an iron oxide catalyst, but scaling up this process remains a challenge. This study shows that ammonia can also be produced from N_2 during a contact process between bulk water and polytetrafluoroethylene (PTFE) particles. This process offers a promising approach for continuous ammonia synthesis on a large scale with low energy consumption under mild conditions.

Ammonia (NH_3) is integral to both agricultural and industrial applications, serving as a foundational element in fertilizers and diverse chemical reactions (1, 2). The synthesis of ammonia is generally achieved by the hydroreduction of nitrogen gas (N_2) in the presence of catalysts (3–5) Currently, the Haber–Bosch process is the dominant method for ammonia synthesis by using fossil fuel-derived hydrogen as the proton donor at high temperatures and pressures, consuming approximately 1.4% of the world's energy supply and emitting close to 400 million tons of CO_2 annually (6–8). Using water (or even humidified air) instead of H_2 as the proton source for ammonia synthesis under room temperature and atmospheric pressure is a green and sustainable alternative to the Haber–Bosch process, which will reduce energy consumption and CO_2 emission during ammonia synthesis (9–13). The task is challenging because the reaction process theoretically requires a constant supply of electrons and protons to activate the nitrogen and subsequent reduction reactions (14). Despite recent developments in ammonia synthesis based on electrocatalysis and photocatalysis, they are often limited by the fact that most protons and electrons in those systems prefer to recombine to produce hydrogen rather than reduce nitrogen (15–17).

Recently, several works have reported that the contact electrification at water–gas interface and water–solid interface can cause electron transfer at their interface and the generation of reactive oxygen species and hydrogen radicals (18–25). The importance of contact electrification for producing radicals has been previously recognized by Grzybowski et al. (26, 27) The contact between water and polytetrafluoroethylene (PTFE) particles, a commercial dielectric material, can catalyze unexpected redox reactions occurring at the interface (28–31). Moreover, recent work has shown that ammonia can generate at the interface between aqueous microdroplets and nitrogen gas, raising hopes for continuous reduction of nitrogen to ammonia during the contact electrification (9). Herein, we describe an approach for ammonia synthesis based on the reaction between protons in water and N_2 adsorbed on the surface of PTFE particles during contact electrification without additional electrical energy or radiation. In this system, ultrasonic waves promote continuous contact between water and solid particles to achieve continuous ammonia synthesis.

Materials and Methods

To investigate whether ammonia can be generated from nitrogen adsorbed on the PTFE surface during the water–solid contact, a reaction system was constructed as shown in Fig. 1*A*. This system consists of three integral components: ultrasonication, temperature control, and gas introduction. A temperature-controlled circulating water system integrated with a copper coil was used to regulate the reaction temperature within the range of 10 to 50 °C. The ultrasonic source operated at a frequency of 40 kHz with an adjustable power output ranging from 0 to 100 W. Gases (nitrogen, air, or nitrogen–oxygen mixtures) were bubbled into the PTFE suspension at 5 kPa, serving as the nitrogen source for the ammonia synthesis. A cylindrical porous mineral bubbler (about

Author affiliations: [a]Hubei Key Laboratory of Environmental and Health Effects of Persistent Toxic Substances, School of Health and Environment, Jianghan University, Wuhan 430056, China; and [b]Department of Chemistry, Stanford University, Stanford, CA 94305

Author contributions: Y.X. and R.N.Z. designed research; J.L., Y.X., and X.S. performed research; J.L., Y.X., B.C., and R.N.Z. analyzed data; and J.L., Y.X., B.C., and R.N.Z. wrote the paper.

Competing interest statement: A patent disclosure has been made to the Stanford Office of Technology Licensing, and the authors declare no other financial conflicts of interest.

This article is a PNAS Direct Submission.

[1]To whom correspondence may be addressed. Email: xiayu@jhun.edu.cn, bl_chen@jhun.edu.cn, or rnz@stanford.edu.

This article contains supporting information online at https://www.pnas.org/lookup/suppl/doi:10.1073/pnas.2318408121/-/DCSupplemental.

Published January 17, 2024.

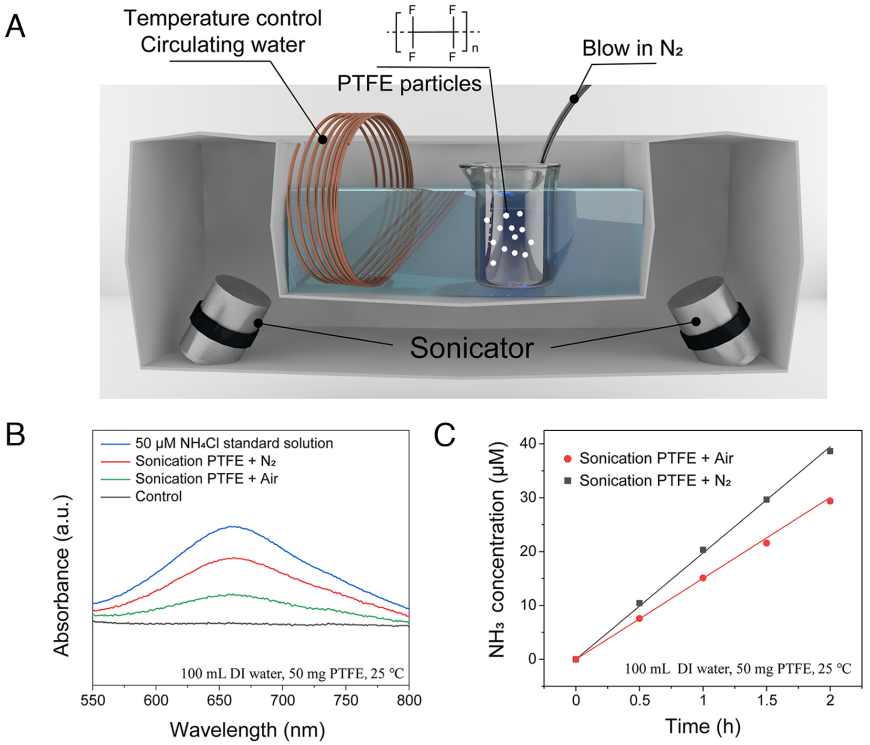

Fig. 1. (*A*) Schematic representation of the experimental setup. (*B*) Absorbance variations using the indophenol blue method under sonication with different atmospheres (100 mL DI water, 50 mg PTFE, 25 °C). (*C*) Comparison of NH_3 yields under air and N_2 at different ultrasonic times performed under the same conditions as in (*B*).

5 cm in diameter) called an air stone is used to create microbubbles of gas. The bubbles that are blown into the sample are not a single large bubble but densely packed with bubbles having diameters ≤500 μm, which results in most contact occurring at the gas–liquid–solid triphasic interfaces, as shown in Movie S1. In addition, the surfactant Tween 20 (<0.05 vol.%) was added to the solution to help the PTFE disperse in the water. It was found that the addition of this surfactant did not appreciably diminish the observed reaction rate.

Results

A quantitative evaluation of the amount of ammonia generated was achieved using the indophenol blue method was undertaken, which results in the dye–ammonium complex exhibiting an absorption peak at 650 nm (12, 13). Standard curves were constructed using ammonium chloride solutions at different concentrations (0, 5, 10, 20, and 30 μM). Using UV–vis spectroscopy, we assessed the ammonia concentration for different ultrasonication durations, as shown in *SI Appendix*, Fig. S1, revealing a linear time-dependent increase in ammonia-dye absorption with increased exposure. Fig. 1*B* illustrates that a sample infused with nitrogen and ultrasonicated for 2 h is superior to using air infusion. Fig. 1*C* shows that ammonia concentration increases linearly with ultrasonication time. Our data also indicate oxygen introduction augments the H_2O_2 concentration while simultaneously decreasing the ammonia concentration (*SI Appendix*, Fig. S2).

To understand better the action of PTFE on the synthesis of ammonia, we investigated the relationship between the mass of PTFE in the suspension and the concentration of ammonia. The results, displayed in Fig. 2*A*, showed that the ammonia yield increases in a nonlinear fashion with increasing PTFE mass, reaching 21 μmol L^{-1} h^{-1} at 50 mg, 31 μmol L^{-1} h^{-1} at 100 mg, 39 μmol L^{-1} h^{-1} at 150 mg, and 43 μmol L^{-1} h^{-1} at 300 mg. Averaging the total ammonia production rate per gram of catalyst, the most efficient and cost-effective performance was observed with 50 mg of the catalyst, which showed a reaction rate of ~420 μmol L^{-1} h^{-1} g^{-1}.

Control experiments were conducted, such as without ultrasonication and instead resorting to mechanical stirring. In the two control groups, it was observed that simply blowing nitrogen into the sample for 1 h without stirring resulted in an ammonia concentration of approximately 3 μmol L^{-1} h^{-1}. In contrast, introducing mechanical stirring while blowing nitrogen for the same duration led to an ammonia concentration nearing 9 μmol L^{-1} h^{-1}. This result indicates that the contact and separation at the triphasic interface (PTFE–water–N_2 gas) plays a key role in the production of ammonia.

We previously discussed the effect of even a slight amount of O_2 on ammonia production (Fig. 1*B*). As a result, the dissolved oxygen in water should be considered. *SI Appendix*, Fig. S3 shows that the yield of ammonia in DI water without deoxygenation is 14 μmol L^{-1} h^{-1}, whereas DI water deoxygenated with nitrogen gas for 30 min yields up to 21 μmol L^{-1} h^{-1} using 50 mg PTFE. Further deoxygenation of 60 min does not increase much the yield, suggesting that 30 min is sufficient to remove dissolved oxygen.

Fig. 2*B* presents data on how the ammonia yield depends on ultrasonic power. The ultrasonic frequency affects the contact frequency between particles and water, while the ultrasonic power controls the intensity of contact between PTFE particles and other molecules. As ultrasonic power increases, the operative distance between molecules decreases, resulting in a concomitant rise in ammonia yield (from 0 to 21 μmol L^{-1} h^{-1}).

The ammonia yield is also influenced by the reaction temperature. As shown in Fig. 2*C*, increasing the temperature from 10 to 25 °C enhances ammonia yield because of a more favorable thermodynamic environment for electron transfer. However, at temperatures exceeding 50 °C, ammonia yield decreases (from 21 to 11 μmol L^{-1} h^{-1}). This decline occurs because the ultrasonic cavitation effect produces highly localized temperatures and pressures. When temperatures in the environment reach high levels, they impede the diffusion of heat, potentially triggering unfavorable electron reactions. Therefore, it is essential to maintain an appropriate temperature to achieve a high yield of ammonia.

In addition, the ammonia yield is closely related to the pH of the PTFE suspension. As shown in Fig. 2*D*, a suspension that is either

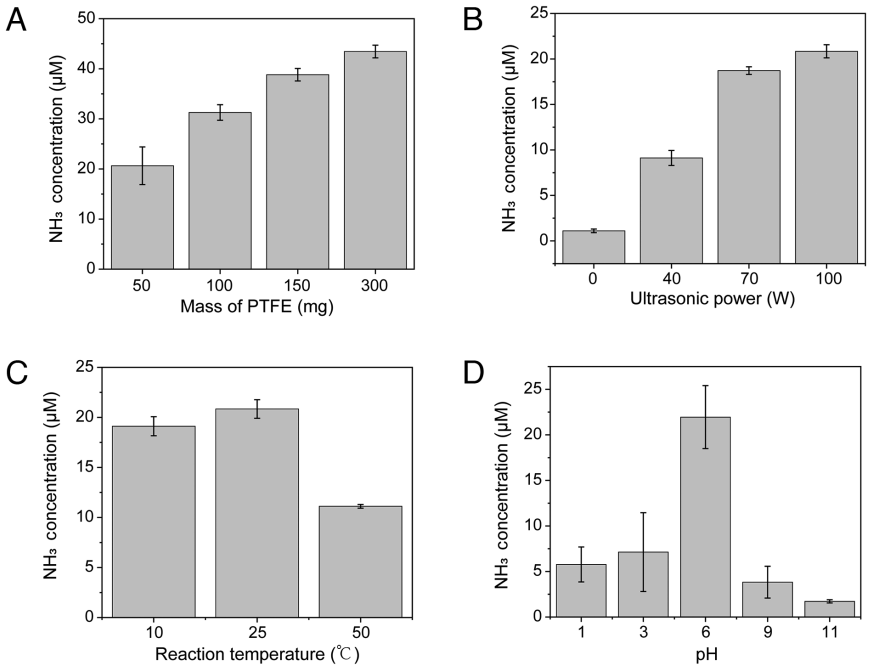

Fig. 2. (*A*) NH_3 generation according to the mass of PTFE added in a 100 mL solution of DI water, at 25 °C. (*B*) NH_3 generation according to the power of the sonication, at 25 °C (100 mL DI water, 50 mg PTFE). (*C*) NH_3 generation according to the reaction temperature (10, 25, and 50 °C) performed under the same conditions as in (*B*). (*D*) NH_3 generation according to pH of PTFE suspension (pH = 1, 3, 6, 9, and 11) performed under the same conditions as in (*B*).

too acidic or too alkaline will adversely affect the ammonia yield. We believe this observation can be attributed to the difference of the arrangement of water molecules at solid surface affected by pH.

Transmission electron microscope energy dispersive spectrometry (TEM-EDS), TEM-Mapping, X-ray photoelectron spectroscopy (XPS) fine spectrum on N1s, mass spectrometry, and NMR characterization related to the ^{15}N isotope experiment were employed to detect reaction products. Nitrogen (N) elements were detected and evenly distributed on the surface of PTFE nanoparticles after the reaction, as shown in *SI Appendix*, Fig. S4*A*. This result indicates that N_2 is adsorbed on PTFE surface for the subsequent reduction reactions. Furthermore, the EDS data in *SI Appendix*, Fig. S4*B* further confirms the existence of nitrogen (N) elements on PTFE. *SI Appendix*, Fig. S4*C* displays fine XPS spectra of N1s that exhibit the adsorption of N_2, NH_3, -NH_2, and -NH on the PTFE surface post-reaction (32, 33). This result suggests that proton hydrogenated N_2 is adsorbed on the solid surface. Moreover, to investigate the reaction mechanism, nitrogen gas was labeled with the isotope ^{15}N. As displayed in *SI Appendix*, Fig. S4*D*, when using $^{14}N_2$, the final product mass spectrum showed a distinct $^{14}NH_4^+$-H_2O (*m/z* = 36) signal. Conversely, upon employing $^{15}N_2$, the *m/z* = 36 signal significantly diminished, while the corresponding $^{15}NH_4^+$-H_2O (*m/z* = 37) signal noticeably intensified (*SI Appendix*, Fig. S4*E*). ^1H-NMR results also confirmed the presence of $^{15}NH_4^+$ in the sample (*SI Appendix*, Fig. S4*F*) (34, 35). These observations offer solid evidence that the generation of ammonia was caused by the reduction of N_2 that has been adsorbed on the PTFE particles.

We conducted experiments using various N_2–O_2 mixtures in the ratio 1:0, 8:2, 5:5, and 0:1. Consistent with previous research, gas-phase oxygen plays a crucial role as a reactant in hydrogen peroxide production (36). Interestingly, samples exposed to ambient air showed a significant increase in hydrogen peroxide concentrations compared to those under pure oxygen. Fig. 3*A* shows that a decrease in the ratio of nitrogen in the N_2–O_2 mixture not only reduces NH_3 production but also leads to a decrease in H_2O_2 production. In addition, using an N_2:O_2 ratio of 8:2 is slightly better than using air as the reactant.

We employed electron paramagnetic resonance spectroscopy to detect radical intermediates. As illustrated in Fig. 3*B*, when nitrogen is the reactant and DMPO is used as the radical trap, our system demonstrated significant signals for $OH^•$ and $H^•$ (37, 38). However, the signal for superoxide radical anions ($O_2^{•-}$) was faint. When the N_2 was switched to a mixture of N_2:O_2 at 8:2 (Fig. 3*C*), we observed signals for $OH^•$ and $O_2^{•-}$, while $H^•$ was noticeably absent.

Based on the above experimental results, we propose a possible reaction mechanism for how ammonia is generated. Ultrasonic treatment enables frequent contact separation between water, nitrogen, and PTFE particles. The overlapping of electron clouds leads to the transfer of electrons from water or nitrogen to the PTFE surface. Additionally, the cavitation effect resulting from ultrasonic treatment can produce localized high pressure, altering the distance between PTFE particles and other molecules, thereby accelerating the contact and separation process between PTFE nanoparticles and other substances. Using density-functional theory (DFT), we have simulated the contact process between water, N_2, and PTFE molecules by examining the effect of different intermolecular distances. *SI Appendix*, Fig. S5*A* illustrates that the band gaps of H_2O/PTFE, N_2/PTFE, and H^+/PTFE* decrease as the intermolecular distance is reduced. It is significant to note that when the distance between the two molecules is reduced by 15% (from without-contact to in-contact), the band gaps decrease by 4.8%, 2.5%, and 5.0% for H_2O/PTFE, N_2/PTFE, and H^+/PTFE*, respectively. Furthermore, *SI Appendix*, Fig. S5*B* shows that the contact process is accompanied by an energy interaction, with values of 4.2, 17.9, and 0.4 kcal/mol, respectively. The above-mentioned DFT calculations offer theoretical evidence in support of electron transfer during the contact process. Thus, we believe that the synthetic ammonia reaction triggered by the contact electrification process can be divided into three steps.

First, water forms hydrogen ions and hydroxide ions at the interface. At the same time, nitrogen is adsorbed on the surface of PTFE, as shown in reactions [**1**] and [**2**].

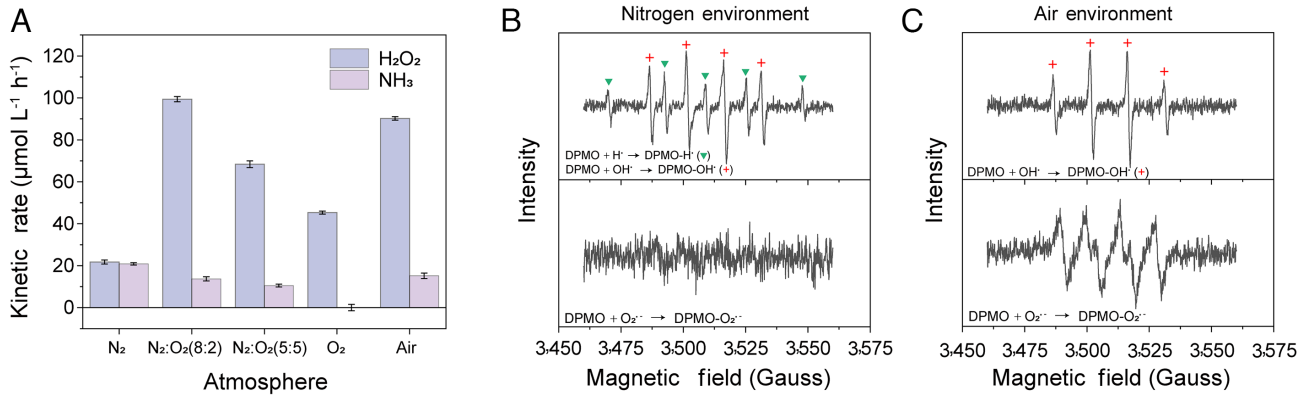

Fig. 3. (*A*) Comparison of kinetic rates of NH_3 generation in PTFE suspensions with different gas components. (*B*) ESR results for N_2 as a reactant in PTFE suspensions including $OH^•$, $H^•$, and $O_2^{•-}$. (*C*) ESR results for N_2–O_2 mixture (8:2) as a reactant in PTFE suspensions including $OH^•$, $H^•$, and $O_2^{•-}$.

$$H_2O \rightarrow H^+ + OH^-, \quad [1]$$

$$PTFE + N_2 \rightarrow PTFE—N_2. \quad [2]$$

Second, promoted by the strong electric field caused by contact electrification at the interface, the hydroxide ion loses an electron to form a hydroxyl radical. Some electrons are trapped by hydrogen ions to form protons (hydrogen radicals), as shown in reactions [**3**] and [**4**].

$$OH^- \rightarrow OH^• + e^-, \quad [3]$$

$$H^+ + e^- \rightarrow H^•. \quad [4]$$

Finally, $H^•$ primarily reacts with the adsorbed nitrogen (PTFE—N_2) in a series of steps to form NH_3, which escapes from the PTFE to regenerate it, as shown in reaction [**5**]. In addition, hydroxyl radicals recombine to hydrogen peroxide, as shown in reaction [**6**].

$$PTFE—N_2 + 6H^• \rightarrow 2NH_3 + PTFE, \quad [5]$$

$$OH^• + OH^• \rightarrow H_2O_2. \quad [6]$$

We compared and studied the difference of synthetic ammonia reaction caused by contact electrification under different pH conditions. As shown in Fig. 2*D*, the ammonia yield is closely related to the pH of the PTFE suspension. A suspension that is either too acidic or too alkaline will adversely affect the ammonia yield. We propose that at acidic pH, the protonation of C-F bonding at the interface is fast, leading to recombination between the H^+ and electron; while at basic pH, the proton can easily diffuse away from the surface. Both above conditions inhibit the reaction between reactive nitrogen adsorbed on PTFE and protons generated during the contact. Therefore, we believe that we can make the electrons and protons react with nitrogen continuously at neutral pH.

Under the established optimal conditions (50 mg of PTFE in 100 mL of deoxygenated DI water, 100 W ultrasonic power, 25 °C), the reaction was run for a total duration of 8 h. As shown in Fig. 4*A*, the ammonia yield remained largely invariant within the initial 4 h. Subsequently, the synthesis rate exhibited a decline, culminating in an almost complete cessation by the end of the 8 h duration. A probable causal factor for this observed trend is the concomitant elevation in the pH of the PTFE suspension as the reaction advanced, which in turn could modulate the reaction kinetics. The pH change of the suspension during the reaction course is detailed in Fig. 4*B*. Concomitant with the reaction's evolution was a discernible increase in the pH of the suspension, potentially serving as the primary determinant governing the reaction rate. To corroborate this postulation, we scrupulously maintained the pH of the suspension within a 6.5 to 7 range, necessitating hourly pH adjustments. With this stringent pH oversight, the ammonia yield (~21 μmol L^{-1} h^{-1}) remained predominantly stable across the 8-h reaction duration, (Fig. 4*C*). This result shows that the ammonia synthesis process based on contact electrification between water and PTFE offers a promising possibility of producing ammonia from the reaction of nitrogen and water continuously under mild conditions. More importantly, our finding holds the promise of replacing the hydrogen gas required for the Haber–Bosch process with water, enabling the ammonia industry to reduce its dependence on fossil fuels for hydrogen production and thereby reducing the industry's carbon dioxide

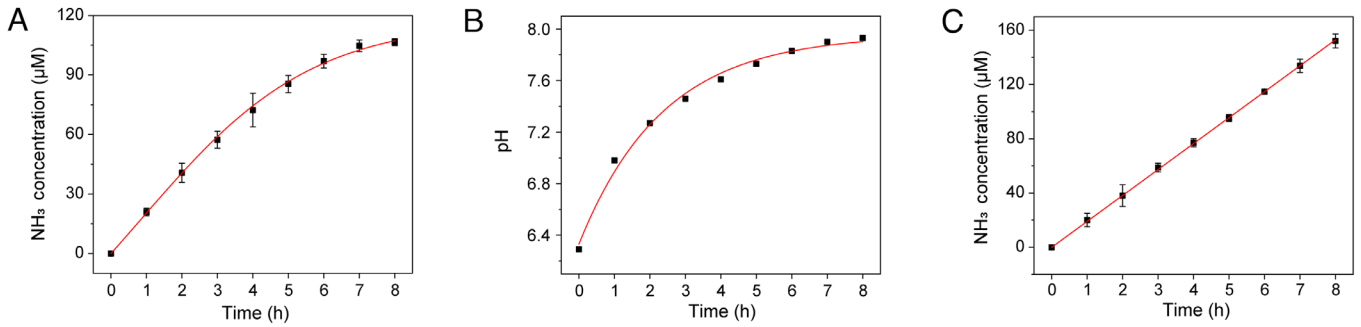

Fig. 4. Fifty milligrams of PTFE in 100 mL of deoxygenated DI water, applying 100 W ultrasonic power, and regulating the reaction temperature approximately at 25 °C. (*A*) The concentration of ammonia in a suspension as a function of reaction time. (*B*) The pH of suspension as a function of reaction time. (*C*) The pH of the suspension was strictly controlled at 6.5 to 7, and the concentration of ammonia in the suspension as a function of reaction time.

emissions on a global scale (which in 2020 was 2.6 t of CO_2 per ton of ammonia) (39).

Conclusion

In this work, we synthesized ammonia from nitrogen gas during the contact between water and PTFE. In this system, N_2 plays a crucial role as the nitrogen source for ammonia, while water acts as the proton donor. ESR (Electron spin resonance) results and DFT simulations demonstrated that radical intermediates regulate the reaction pathway, offering a perspective on the autonomous control of radical reactions in-contact electrocatalysis. Moreover, by optimizing experimental parameters and comparing the oxidative and reductive products (H_2O_2 and NH_3) under varying conditions, we have found some general principles affecting contact electrocatalysis. By strictly controlling the pH of the suspension, we also demonstrated that this method can continuously generate ammonia over an 8-h period without any appreciable change in the reaction rate. Our findings deepen the understanding of contact electrocatalysis and suggest its possible use in scaling up such reactions.

Data, Materials, and Software Availability. All study data are included in the article, the supporting information, and the publicly available link: https://github.com/YuXia19/Continuous-ammonia-synthesis-from-water-and-nitrogen-via-contact-electrification (40).

ACKNOWLEDGMENTS. This work represents a collaboration in which work at Jianghan University was financially supported by the National Natural Science Foundation of China (22306073, 22376080, and 22193051) and work at Stanford University by the US Air Force Office of Scientific Research through the Multidisciplinary University Research Initiative program (AFOSR FA9550-21-1-0170).

1. A. Valera-Medina, H. Xiao, M. Owen-Jones, W. I. F. David, P. J. Bowen, Ammonia for power. *Prog. Energy Combust. Sci.* **69**, 63–102 (2018).
2. R. Dunn, K. Lovegrove, G. Burgess, A review of ammonia-based thermochemical energy storage for concentrating solar power. *Proc. IEEE* **100**, 391–400 (2012).
3. M. J. Chalkley, M. W. Drover, J. C. Peters, Catalytic N_2-to-NH_3 (or -N_2H_4) conversion by well-defined molecular coordination complexes. *Chem. Rev.* **120**, 5582–5636 (2020).
4. Q. Liu *et al.*, Recent advances in strategies for highly selective electrocatalytic N_2 reduction toward ambient NH_3 synthesis. *Curr. Opin. Electrochem.* **29**, 100766 (2021).
5. G.-F. Chen *et al.*, Advances in electrocatalytic N_2 reduction–Strategies to tackle the selectivity challenge. *Small Methods* **3**, 1800337 (2019).
6. J. Guo, P. Chen, Catalyst: NH_3 as an energy carrier. *Chem* **3**, 709–712 (2017).
7. G. N. Schrauzer, T. D. Guth, Photolysis of water and photoreduction of nitrogen on titanium dioxide. *J. Am. Chem. Soc.* **99**, 7189–7193 (1977).
8. W. Qiu *et al.*, High-performance artificial nitrogen fixation at ambient conditions using a metal-free electrocatalyst. *Nat. Commun.* **9**, 3485 (2018).
9. X. Song, C. Basheer, R. N. Zare, Making ammonia from nitrogen and water microdroplets. *Proc. Natl. Acad. Sci. U.S.A.* **120**, e2301206120 (2023).
10. H. Xu *et al.*, Electrochemical ammonia synthesis through N_2 and H_2O under ambient conditions: Theory, practices, and challenges for catalysts and electrolytes. *Nano Energy* **69**, 104469 (2020).
11. G. Zhang *et al.*, Recent progress in 2D catalysts for photocatalytic and electrocatalytic artificial nitrogen reduction to ammonia. *Adv. Energy Mater.* **11**, 2003294 (2021).
12. I. Muzammil *et al.*, Plasma catalyst-integrated system for ammonia production from H_2O and N_2 at atmospheric pressure. *ACS Energy Lett.* **6**, 3004–3010 (2021).
13. X. Fu *et al.*, Continuous-flow electrosynthesis of ammonia by nitrogen reduction and hydrogen oxidation. *Science* **379**, 707–712 (2023).
14. C. J. M. van der Ham, M. T. M. Koper, D. G. H. Hetterscheid, Challenges in reduction of dinitrogen by proton and electron transfer. *Chem. Soc. Rev.* **43**, 5183–5191 (2014).
15. M. Li *et al.*, Recent progress on electrocatalyst and photocatalyst design for nitrogen reduction. *Small Methods* **3**, 1800388 (2019).
16. X. Xue *et al.*, Review on photocatalytic and electrocatalytic artificial nitrogen fixation for ammonia synthesis at mild conditions: Advances, challenges and perspectives. *Nano Res.* **12**, 1229–1249 (2019).
17. Z. Yan, M. Ji, J. Xia, H. Zhu, Recent advanced materials for electrochemical and photoelectrochemical synthesis of ammonia from dinitrogen: One step closer to a sustainable energy future. *Adv. Energy Mater.* **10**, 1902020 (2020).
18. B. Chen *et al.*, Water–solid contact electrification causes hydrogen peroxide production from hydroxyl radical recombination in sprayed microdroplets. *Proc. Natl. Acad. Sci. U.S.A.* **119**, e2209056119 (2022).
19. D. Xing *et al.*, Capture of hydroxyl radicals by hydronium cations in water microdroplets. *Angew. Chem. Int. Ed. Engl.* **61**, e202207587 (2022).
20. Y. Xia *et al.*, Contact between water vapor and silicate surface causes abiotic formation of reactive oxygen species in an anoxic atmosphere. *Proc. Natl. Acad. Sci. U.S.A.* **120**, e2302014120 (2023).
21. D. Zhang, X. Yuan, C. Gong, X. Zhang, High electric field on water microdroplets catalyzes spontaneous and ultrafast oxidative C-H/N–H cross-coupling. *J. Am. Chem. Soc.* **144**, 16184–16190 (2022).
22. X. Yuan, D. Zhang, C. Liang, X. Zhang, Spontaneous reduction of transition metal ions by one electron in water microdroplets and the atmospheric implications. *J. Am. Chem. Soc.* **145**, 2800–2805 (2023).
23. H. Chen *et al.*, Spontaneous reduction by one electron on water microdroplets facilitates direct carboxylation with CO_2. *J. Am. Chem. Soc.* **145**, 2647–2652 (2023).
24. C. Gong *et al.*, Spontaneous reduction-induced degradation of viologen compounds in water microdroplets and its inhibition by host–guest complexation. *J. Am. Chem. Soc.* **144**, 3510–3516 (2022).
25. S. Jin *et al.*, The spontaneous electron-mediated redox processes on sprayed water microdroplets. *JACS Au* **3**, 1563–1571 (2023).
26. B. Baytekin, H. T. Baytekin, B. A. Grzybowski, What really drives chemical reactions on contact charged surfaces? *J. Am. Chem. Soc.* **134**, 7223–7226 (2012).
27. Z. Yang, Q. Zhuang, Y. Yan, G. Ahumada, B. A. Grzybowski, An electrocatalytic reaction as a basis for chemical computing in water droplets. *J. Am. Chem. Soc.* **143**, 16908–16912 (2021).
28. Z. Wang *et al.*, Contact-electro-catalysis for the degradation of organic pollutants using pristine dielectric powders. *Nat. Commun.* **13**, 130 (2022).
29. X. Dong *et al.*, Investigations on the contact-electro-catalysis under various ultrasonic conditions and using different electrification particles. *Nano Energy* **99**, 107346 (2022).
30. A. Berbille *et al.*, Mechanism for generating H_2O_2 at water-solid interface by contact-electrification. *Adv. Mater.* **35**, e2304387 (2023).
31. J. Zhao *et al.*, Contact-electro-catalysis for direct synthesis of H_2O_2 under ambient conditions. *Angew. Chem. Int. Ed. Engl.* **62**, e202300604 (2023).
32. Y. Wang *et al.*, Plasma-enhanced catalytic synthesis of ammonia over a Ni/Al_2O_3 catalyst at near-room temperature: Insights into the importance of the catalyst surface on the reaction mechanism. *ACS Catal.* **9**, 10780–10793 (2019).
33. I. Louis-Rose, C. Méthivier, J. C. Védrine, C.-M. Pradier, Reduction of N_2O by NH_3 on polycrystalline copper and Cu(110): A combined XPS, FT-IRRAS and kinetics investigation. *Appl. Catal. B Environ.* **62**, 1–11 (2006).
34. J. Lee *et al.*, Phase-selective active sites on ordered/disordered titanium dioxide enable exceptional photocatalytic ammonia synthesis. *Chem. Sci.* **12**, 9619–9629 (2021).
35. S. Z. Andersen *et al.*, A rigorous electrochemical ammonia synthesis protocol with quantitative isotope measurements. *Nature* **570**, 504–508 (2019).
36. M. A. Mehrgardi, M. Mofidfar, R. N. Zare, Sprayed water microdroplets are able to generate hydrogen peroxide spontaneously. *J. Am. Chem. Soc.* **144**, 7606–7609 (2022).
37. X. Chen *et al.*, Hydrocarbon degradation by contact with anoxic water microdroplets. *J. Am. Chem. Soc.* **145**, 21538–21545 (2023).
38. K. P. Madden, H. Taniguchi, The role of the DMPO-hydrated electron spin adduct in DMPO-OH spin trapping. *Free Radical Biol. Med.* **30**, 1374–1380 (2001).
39. World Economic Forum, Net-zero industry tracker 2023 edition (2023). https://www3.weforum.org/docs/WEF_Net_Zero_Tracker_2023_REPORT.pdf.
40. Y. Xia, YuXia19/Continuous-ammonia-synthesis-from-water-and-nitrogen-via-contact-electrification. Github. https://github.com/YuXia19/Continuous-ammonia-synthesis-from-water-and-nitrogen-via-contact-electrification. Deposited 23 December 2023.